

## Parametric motion of energy levels in quantum chaotic systems. II. Avoided-crossing distributions

Jakub Zakrzewski\* and Dominique Delande

*Laboratoire de Spectroscopie Hertzienne de l'École Normale Supérieure, Université Pierre et Marie Curie, T12-E1,  
4 place Jussieu, 75272 Paris CEDEX 05, France*

Marek Kuś

*Centrum Fizyki Teoretycznej, Polish Academy of Sciences, Aleja Lotnikow 32/46, Warsaw, Poland*

(Received 6 October 1992)

Statistical properties of levels of quantum systems chaotic in the classical limit are studied using the distribution of avoided crossings, i.e., of the sizes of local minima of adjacent-level spacings. The results obtained previously for the two-level random-matrix theory are compared with the predictions of the statistical-mechanics description of the equivalent fictitious-particle system. The distributions derived are compared with numerical results obtained for several physical systems. The origin of the discrepancies (in former numerical calculations) of small-avoided-crossing behavior is found. The ratio of the average crossing to the average spacing is shown to have a nonuniversal behavior and seems to provide information on the degree of scarring in the system studied.

PACS number(s): 05.40.+j, 05.45.+b

### I. INTRODUCTION

This paper is a continuation of our study of the statistical properties of the motion of the energy levels in quantally chaotic systems when some parameter describing the system, say  $\lambda$ , is varied. While in the preceding paper [1], referred to here as I, we considered the distribution of curvatures, i.e., the second derivatives of energy levels with respect to  $\lambda$ , we shall concentrate here on the properties of the so-called avoided crossings. We attempted to make this paper as self-contained as possible. However, to avoid excessive repetitions, we shall frequently refer to the results obtained in I. In particular, Eq. (2.1) of I will be referred to simply as Eq. (I.2.1).

Consider the motion of energy levels in a generic system as a parameter  $\lambda$  is varied. By an avoided crossing we mean any local minimum in the distance between the adjacent energy levels. The distribution of avoided crossings is defined as the distribution of the avoided-crossing gaps, i.e., of the minimal distances between the adjacent levels.

The appearance of a multitude of avoided crossings was identified already as a hallmark of the irregular behavior in a quantum system a long time ago [2]. While this finding became quite commonly accepted, little had been done to classify quantitatively the behavior of avoided crossings in a generic quantally chaotic system until the pioneering work of Wilkinson [3]. He derived the analytical expressions for the number of small avoided crossings in a given system (in the limit of vanishingly small crossings) using the random-matrix theory (RMT) [4–7]. It has been predicted that the number of crossings with value less than  $C$  grows linearly with  $C$  for the orthogonal universality class of systems [the corresponding ensemble of random matrices is called the Gaussian orthogonal ensemble (GOE)] and quadratically for systems that belong

to the unitary class [Gaussian unitary ensemble (GUE)]. These results were found to disagree [8] with the numerically calculated small-avoided-crossing distributions for two model systems: the so-called Africa billiard (so named because of its shape) and the hydrogen atom in a strong magnetic field.

The avoided-crossing distribution is an interesting quantity to study due to its statistical properties in relation to the parametric motion of levels. Probably even more importantly is its application, e.g., in the study of the applicability range of the adiabatic theory. The presence of a large number of very small avoided crossings, as implied by [3], would mean that the adiabatic approach for strongly chaotic systems belonging to the orthogonal universality class must be very difficult to apply. By contrast, the presence of the small crossings hole in the distribution, if confirmed, would provide a hope for such an approach. Avoided crossings appear quite naturally, for example, in the study of atomic systems perturbed by external fields, in treating the molecular systems as a function of the internuclear distance, etc. Knowledge of their generic behavior is, therefore, quite important.

The nearest-neighbor-spacing distribution for random ensembles [GOE, GUE, and the third universality class, the symplectic case, for which the corresponding ensemble is called Gaussian symplectic ensemble (GSE)] are very well approximated by the famous Wigner surmise [4–7] obtained by considering  $2 \times 2$  matrices. As shown by us in a recent Letter [9], a similar approach enables one to obtain simple analytic expressions for the distribution of avoided crossings for all three universality classes. The analytic formulas were found to be in very good agreement with distributions obtained via numerical experiments [9] on the kicked-top model [10–12].

The aim of the present paper is to discuss in more detail the distribution of avoided crossings for systems

which exhibit chaotic behavior in the classical limit. In Sec. II, the theoretical results of our previous short report on this work [9] are reviewed. New formulas for the distribution of avoided crossings are found using the statistical-mechanics approach to the motion of levels described by an equivalent Hamiltonian of fictitious interacting particles. Although the calculations are also limited to a two-level simplified model, we find small differences between the results presented here and the former expressions [9]. The origin of these differences is pointed out. It is shown that the present formulas reduce, in the limit of very small crossings, to the original expression of Wilkinson [3] after an appropriate rescaling of small-spacing behavior. We discuss also the relation between the average crossing size and the average spacing for all three universality classes.

The theoretical predictions are compared with the numerical data in Sec. III. The rich variety of systems are studied including a model random-matrix dynamics introduced in I, the kicked-top model, the hydrogen atom in a magnetic field as well as the Africa billiard. More importantly we find that the “hole” present in the previous evaluations of avoided-crossing distributions for the hydrogen atom in a strong magnetic field and the Africa billiard [8] and later confirmed for the kicked top [9] is a spurious effect resulting from the numerical procedure adopted in both these papers. The results obtained are shown to agree qualitatively with the limiting expressions of [3] as well as with the full distributions predicted in [9] and in Sec. II.

Finally, in the concluding Sec. IV we summarize the results obtained. We find that the ratio of the average crossing to the average spacing is a nonuniversal quantity which provides a crude estimate of the degree of “scarring” [13] in the system. We discuss the relation between the statistical properties of curvatures discussed in I and that of the avoided crossings.

## II. AVOIDED CROSSINGS IN TWO-LEVEL MODELS OF DYNAMICS

### A. $H_1 + \lambda H_2$ dynamics—RMT predictions [9]

Consider a system dependent on a parameter  $\lambda$ ,

$$H(\lambda) = H_1 + \lambda H_2. \quad (2.1)$$

We prefer the notation of Eq. (2.1) over the more standard form  $H = H_0 + \lambda V$ , as the latter is frequently used in situations for which  $V$  is a perturbation of typically integrable  $H_0$ . This is not the case considered here. As mentioned in I, we assume that in the full range of  $\lambda$  the classical motion corresponding to  $H$  is strongly chaotic. Moreover, we assume that the change in  $\lambda$  does not modify the symmetries of  $H$ , i.e., the system preserves its character with respect to the main universality classes as defined in RMT [4–7]; see also I.

It is possible to obtain simple analytic formulas for these distributions assuming that the avoided crossings are isolated, i.e., involve two levels only and are well separated on the energy and/or parameter scale from each other. Actually, one may make a weaker assumption,

namely, that multiple avoided crossings, i.e., avoided crossings which involve at least three levels, appear less frequently and are, therefore, statistically insignificant [9]. Then one may consider, locally, only the two strongly interacting levels which reduces the problem to the  $2 \times 2$  ( $4 \times 4$  for the symplectic system) Hamiltonian matrices. A similar approach for the nearest-neighbor spacing distributions leads to the Wigner surmise yielding an excellent approximation to the exact RMT spacings distributions for all three universality classes [6, 7].

The avoided-crossing distributions are particularly easy to obtain in the basis in which  $V$  is diagonal. In the  $2 \times 2$  subspace the effective Hamiltonian may be represented (for GOE and GUE) as

$$H = \begin{bmatrix} a & c \\ c & b \end{bmatrix} + \lambda \begin{bmatrix} v_1 & 0 \\ 0 & v_2 \end{bmatrix}. \quad (2.2)$$

In Eq. (2.2),  $a$ ,  $b$ ,  $v_1$ , and  $v_2$  are real numbers. Simple calculation shows that the value of the avoided crossing (i.e., the minimal gap between the energy levels as a function of  $\lambda$ ) is  $C = 2|c|$ .

For GOE,  $c$  is real and normally distributed,

$$P(c) = \sqrt{\pi}\sigma \exp(-c^2/\sigma^2), \quad (2.3)$$

according to RMT [4–7].

Then the probability distribution of avoided crossings reads

$$P_O(C) = \sqrt{\pi}\sigma \exp\left(-\frac{C^2}{4\sigma^2}\right), \quad C > 0, \quad (2.4)$$

while a standard  $2 \times 2$  calculation for the spacing  $S$  distribution (see, e.g., [6]), assuming  $H(\lambda)$  pertains to GOE, yields

$$P(S) = \frac{1}{2\sigma^2} S \exp\left(-\frac{S^2}{4\sigma^2}\right), \quad (2.5)$$

which leads to the unit average spacing for  $\sigma^2 = \pi^{-1}$ . With this  $\sigma^2$  value, Eq. (2.4) gives the average crossing value equal to  $\bar{C} = 2/\pi$ .

One may also, as we have done in [9], represent Eq. (2.4) in the form normalized to the unit average avoided crossing,

$$P_O(C) = \frac{2}{\pi} \exp\left(-\frac{C^2}{\pi}\right), \quad C > 0. \quad (2.6)$$

There is a certain flaw in the arguments given above. For any particular realization of  $H_1$  and  $H_2$  in Eq. (2.1), the levels separate with an increase of  $\lambda$  for a sufficiently large  $\lambda$ . Thus the calculation of spacing distribution is valid in the limit of small  $\lambda$  only while the crossing distribution is calculated regardless of the  $\lambda$  value. The comparison of the spacing distribution and the crossing distribution given above, and in particular the obtained ratio of the average crossing to the average spacing  $\bar{C} = 2/\pi$ , is, therefore, falsified. One should first unfold the levels and then compute the crossings; this requires knowledge of the crossings position with respect to  $\lambda$  for each realization of the Hamiltonian matrix. Such a procedure is quite complicated and a better approach to this problem will be presented below.

It is quite obvious, however, that the majority of crossings may appear in the  $2 \times 2$  matrix model with linear dependence on  $\lambda$  only for  $\lambda$  small. Once  $\lambda$  becomes large, the spacing generally increases and a probability for a local minimum in the spacing becomes negligible. We expect, therefore, that the distribution given by Eq. (2.6) above and by Eqs. (2.7), (2.9), and (2.11) below for other universality classes should to a large extent resemble the "exact" distributions which take into account the necessary unfolding. The appropriate ratio of the average crossing to the average spacing valid for the  $2 \times 2$  model cannot be, however, obtained in this way.

In the GUE case  $c$  is a complex number  $c = c_R + ic_I$  where, according to RMT,  $c_R$  and  $c_I$  are independently normally distributed with the same dispersion. Simple calculation then yields [9]

$$P_U(C) = \frac{\pi C}{2} \exp\left(-\frac{\pi}{4}C^2\right), \quad (2.7)$$

choosing such a  $\sigma$  value that the average avoided crossing is equal to one.

It is interesting to study the case when the orthogonal symmetry of  $H$  is partially broken only [14]. Such a situation may be realized in our simple model assuming that the dispersion  $\sigma_I$  of  $c_I$  is smaller than  $\sigma_R$  of  $c_R$

$$\sigma_I^2 = \alpha \sigma_R^2. \quad (2.8)$$

Changing  $\alpha$  from 0 to 1 allows us to study a whole family of systems from pure GOE case ( $\alpha = 0$ ) to pure GUE systems ( $\alpha = 1$ ). Note that the change of  $\lambda$  does not correspond to the change of the symmetry as in [14]. The calculation of probability distribution of avoided crossings proceeds as in (2.7) above. The integration is slightly more difficult due to different dispersions of  $P(c_R)$  and  $P(c_I)$  and gives

$$P(C) = \frac{A(\alpha)}{2\sqrt{\alpha}} C \exp\left(-\frac{(1+\alpha)A(\alpha)}{8\alpha}C^2\right) \times I_0\left(\frac{(1-\alpha)A(\alpha)}{8\alpha}C^2\right) \quad (2.9)$$

with  $A(\alpha)$  given by

$$A(\alpha) = \frac{16\alpha}{\pi(1-\alpha)} \left[ Q_{-1/2}^1\left(\frac{1+\alpha}{1-\alpha}\right) \right]^2. \quad (2.10)$$

Following [15],  $I_0$  denotes the modified Bessel function while  $Q_{-1/2}^1$  is the associated Legendre function of the second kind.

The GSE case is only slightly different in a sense that the eigenvalues should appear in pairs (Kramers degeneracy [6]) and we have to consider a  $4 \times 4$  Hamiltonian (symplectic) matrix (for details see [9]). The distribution of avoided crossings may be expressed as

$$P_S(C) = \frac{81\pi^2}{128} C^3 \exp\left(-\frac{9\pi}{16}C^2\right) \quad (2.11)$$

again, for the average avoided crossing equal to one.

## B. Statistical-mechanics predictions

The above-mentioned problem of unfolding the levels is easily overcome by modifying the dependence of the total Hamiltonian on  $\lambda$ . Assume it takes the form (see I)

$$H(\lambda) = \cos(\lambda)H_1 + \sin(\lambda)H_2, \quad (2.12)$$

which reduces to Eq. (2.1) in the important region of  $\lambda$  small. If we now assume that  $H_1$  and  $H_2$  belong to the same universality class and have the same mean spacing, the mean spacing of  $H$  in Eq. (2.12) becomes independent of  $\lambda$ . One could, therefore, improve the approach presented above by considering the crossing distribution using a similar method applied to the  $\lambda$  dependence given by Eq. (2.12). The resulting calculations are quite tiresome algebraically; we shall in the following use a statistical-mechanics approach, similar to that used for the curvature studies in I. For  $2 \times 2$  matrices both approaches are, however, equivalent.

To this end we consider the dynamics of the fictitious interacting particles model corresponding to Eq. (2.12) (for details the reader is advised to consult Secs. II and III A of I) described by the Hamiltonian given by Eq. (I.3.3). We use the canonical ensemble defined by the Gibbs measure  $dG_N$ , Eq. (I.3.6), where  $N$  is the number of levels in the system. We restrict ourselves in the following to the  $N = 2$  model for simplicity.

Avoided crossings, as minima of the spacing between the two levels considered, appear at certain values of parameter  $\lambda$ ,  $\lambda = \lambda_i$ . Therefore the number of avoided crossings with size  $C$  per unit interval of  $\lambda$  values may be found as

$$n(C) = \sum_i \int dG_2 \delta(\lambda - \lambda_i) \delta(C - |x_1 - x_2|), \quad (2.13)$$

where, as in I,  $x_k$  denotes the energy of the  $k$ th level,  $k = 1, 2$ . To evaluate the integral above it is convenient to reexpress the  $\delta(\lambda - \lambda_i)$  in terms of the slopes of the levels,  $p_k = dx_k/d\lambda$ , i.e., the momenta of fictitious particles. Their motion is governed by Eq. (I.3.5). One immediately notices that at any avoided crossing the momenta of the levels involved in the crossing must be equal, i.e.,  $p_1 = p_2$ . Moreover, the curvature of the higher-lying level must be larger than that of the lower level (the opposite case corresponds to the local maximum of the spacing). Therefore

$$\sum_i \delta(\lambda - \lambda_i) = \delta(p_1 - p_2) \frac{d(p_1 - p_2)}{d\lambda} \quad (2.14)$$

with the understanding that for  $x_1 - x_2 > 0$  ( $< 0$ ) the domain of integration in Eq. (2.13) is restricted to positive (negative) values of the derivative in Eq. (2.14). Substitution of Eq. (2.14) into Eq. (2.13) yields a general formula which may be easily generalized for arbitrary  $N$ . We were not able, however, to evaluate the resulting integrals for arbitrary  $N$  values.

On the other hand, for the  $N = 2$  model, the integration is quite straightforward for all three universality classes. We obtain for the orthogonal (GOE) system

$$n_O(C) = \frac{\sqrt{\beta}}{2\pi} \exp\left(-\frac{\beta C^2}{4}\right) \times \left[ \sqrt{\beta} C \exp\left(-\frac{\beta C^2}{4}\right) + \sqrt{\pi} \operatorname{erfc}\left(\sqrt{\beta} C/2\right) \left(1 - \frac{\beta C^2}{2}\right) \right], \quad (2.15)$$

where  $\beta$  is the inverse temperature in the canonical measure and determines the density of states (see I).

The total number of crossings in the unit interval of  $\lambda$  is given by

$$n_O^T = \int_0^\infty dC n_O(C) = \frac{1}{\pi} \quad (2.16)$$

and is independent of  $\beta$ . The above result has the sense of the average over the canonical distribution. Using explicitly the periodicity of Eq. (2.12) with the period  $T = \pi$  one may easily prove a stronger statement, namely that for any single realization of  $2 \times 2$  matrices  $H_1$  and  $H_2$ , one will have exactly one minimum and one maximum of the spacing per period. The identical result is obtained for the GUE and the GSE cases and easily confirmed by the integration of the corresponding expressions for  $n_U(C)$ , Eq. (2.19), and  $n_S(C)$ , Eq. (2.20).

As mentioned in I, the canonical ensemble yields for arbitrary  $N$  the same joint probability density of levels as the RMT. In particular, one may derive from it the Wigner surmise for the  $2 \times 2$  matrix nearest-neighbor-spacing distribution. For the GOE case, the unit spacing corresponds to  $\beta = \pi$ , independently of  $\lambda$  (stationarity of the ensemble—see I). The average crossing to the average spacing ratio may be now obtained using Eq. (2.15) with the norm given by  $n_0^T$

$$\bar{C}_O = \sqrt{2} - 1. \quad (2.17)$$

It is interesting to compare the number of crossings of smaller size than some small  $C_m$ , obtained from Eq. (2.15) for the two-levels model with unit spacing,

$$n_2 = \int_0^{C_m} dC n_O(C) \approx C_m \frac{1}{2} \sqrt{\frac{\pi}{\beta}} \quad (2.18)$$

with the similar quantity derived in the large- $N$  limit by Wilkinson [3] which, in our notation, takes the form  $n_\infty = C_m \pi^{3/2} / 6\sqrt{\beta}$ . The ratio of  $n_2$  to  $n_\infty$  is equal to the ratio of leading coefficients in the spacing distribution of the Wigner surmise for GOE ( $\pi/2$ ) to the exact formula valid for large  $N$  [4–7] ( $\pi^2/6$ ). This is easily understood as the smallest crossings are well described by the two-level model.

Equally easy calculations yield the number of crossings of size  $C$  for the GUE and the GSE systems. Explicitly we obtain in the units of the mean average spacing in the GUE case

$$n_U(C) = \frac{16C}{\pi} \exp(-8C^2/\pi) \quad (2.19)$$

with the average crossing equal to  $\bar{C}_U = \pi/4\sqrt{2}$ . For the GSE we obtain in the same units

$$n_S(C) = \frac{2^{16}C^3}{3^5\pi^3} \left(1 + \frac{2^5C^2}{9\pi}\right) \exp(-2^7C^2/9\pi) \quad (2.20)$$

and the average crossing  $\bar{C}_S = 39\pi/128\sqrt{2}$ .

For the direct comparison with the formulas obtained before [9] for the  $2 \times 2$  model linearly dependent on  $\lambda$  [Eqs. (2.6), (2.7), and (2.11)] the present expressions given by Eqs. (2.15), (2.19), and (2.20) should be represented in the units of mean average crossing. It is, however, clear from their functional dependence that there are some differences in the GOE and GSE cases, while for the GUE the functional form is the same. We will compare the corresponding distributions while analyzing the numerical data for various systems in Sec. III. Let us mention only that the difference is quite small, which supports the claim given at the end of Sec. II A, namely that the former formulas [9], although found without unfolding the levels, provide a good approximation for the crossing distributions for the  $2 \times 2$  model in units of the mean crossing.

On the other hand, as mentioned there also, the average crossing values obtained using the previous approach are wrong and the correct predictions of the two-level dynamics are the one given by the values of  $\bar{C}_O$ ,  $\bar{C}_U$ , and  $\bar{C}_S$  given above.

### III. NUMERICAL STUDIES

In a previous Letter [9] we have compared the distributions (2.6), (2.7), (2.9), and (2.11) with numerical data obtained in several versions of the kicked-top model [11]. Very good agreement has been found for all three universality classes in general. There were, however, significant differences for the orthogonal case in the limit of small avoided crossings similar to that found in [8] for other systems. Starting with the orthogonal class systems, we shall in this section first reevaluate the data for the orthogonal kicked top and show that the effect previously observed was a spurious one resulting from the inaccuracy of the numerical procedure adopted in [8, 9]. Then we shall consider a “generic” model based on RMT, introduced already in detail in I. Later, we compare the theoretical expressions with the data for the Africa billiard [8] and the hydrogen atom in a strong magnetic field. In Sec. III B we shall consider also the predictions of the “generic” random model for other universality classes.

#### A. Orthogonal universality class systems

##### 1. Kicked-top revisited

The kicked-top (KT) model system has been shown [10–12] to follow quite remarkably the predictions of RMT concerning the statistical properties of both eigenvalues and eigenvectors. It was thus quite a surprise for us when we found numerically [9] that the small avoided crossings appear in this system in a much smaller relative number than that predicted by the RMT expression, Eq. (2.6). On the other hand, this finding correlated well with a previous report [8] in which the similar small-

crossing “hole” has been found for both the Africa billiard and the hydrogen atom in a strong magnetic field. Here, we reexamine the numerical procedure used to find the values of the crossings.

The kicked top belongs to the class of time-dependent systems in which an integrable Hamiltonian is perturbed periodically by very short and strong perturbations modeled by the  $\delta$  function—the so-called  $\delta$  kicks. For such systems, properties of the evolution operator over one period of the perturbation rather than properties of the Hamiltonian itself are of interest. The evolution operator we consider reads [11, 9]

$$U = \exp(-ipJ_y) \exp\left(-i\frac{k}{2j}J_z^2\right), \quad (3.1)$$

where  $J_y$  and  $J_z$  are the  $(2j+1) \times (2j+1)$  spin matrices and  $p$  and  $k$  are the parameters. We can choose either  $k$  or  $p$  as the coupling parameter  $\lambda$ . In the numerical calculations we change  $\lambda = p$  in intervals where the classical motion is fully chaotic.

The numerical procedure to evaluate the avoided crossings seems straightforward. It is sufficient to diagonalize Eq. (3.1) in sufficiently small steps in  $\lambda = p$  and find the local minima in the distance between the eigenphases of  $U$  (eigenvalues lie obviously on the unit circle). Strictly speaking the corresponding ensemble of random matrices is not GOE but rather the circular orthogonal ensemble, but this does not affect the predictions of RMT [6, 7, 14]. Instead of using numerically found minima, one may interpolate the eigenphases between consecutive diagonalizations to obtain the improved values of the avoided crossings sizes.

The procedure adopted in [8], and followed by us before [9], was to make a parabola fit to the result of three consecutive diagonalizations for each level independently. A quite natural criterion of the convergence of this procedure appears: one assumes avoided crossings sizes are properly estimated when the fitted values of the crossings do not differ much from the corresponding values obtained using just the diagonalization data. As any curve can be locally represented by the Taylor series expansion to the second order, this approach seems to be quite accurate. However, this is not the end of the story, as otherwise we could not improve over the results presented before.

In fact, explicit calculation for a  $2 \times 2$  model shows easily [3] that the dependence of the levels (here eigenphases) on the parameter  $\lambda$  has the form of a hyperbola, whose branches describe the two levels undergoing the avoided crossings. It is easy to show that the same data, i.e., three consecutive distances  $d_i$ ,  $i = 1, 2, 3$ , between the adjacent levels (of which the middle one is the smallest) are sufficient to determine precisely the minimal distance between the levels  $C$ , assuming the hyperbola dependence on  $\lambda$ . One easily gets

$$C = \sqrt{d_2^2 - \frac{(d_3^2 - d_1^2)^2}{8(d_3^2 + d_1^2 - 2d_2^2)}}, \quad (3.2)$$

where the denominator should be positive [this is a requirement for a local minimum, compare Eq. (2.14)]. Us-

ing Eq. (3.2) we have reevaluated the avoided crossings sizes using similar parameters and, importantly, a similar step in  $\lambda$  as in [9]. We found that the results of the “parabola fit” and the “hyperbola fit” differ significantly for the very small (much smaller than the average crossing—see below) crossings. Moreover, for about 50 out of roughly 10 000 crossings, the value of  $C$  obtained has been imaginary (the argument under the square root is negative).

We have, therefore, decreased the step size in the diagonalization and we have noticed that the number of “imaginary” crossing sizes decreased significantly. More importantly, while the numerical values of the hyperbola fitted avoided crossings sizes have been only slightly modified, some values of the smallest parabola fitted crossings decreased sharply (although in both cases they have been very close to the values obtained from direct diagonalization data). It has become quite clear that the numerical procedure adopted in [8, 9] has not been the best. Figure 1 presents the results on the global scale. The normalized histogram of avoided crossings on this scale, and due to the finite size of the bin, does not differ within the statistical deviation from the corresponding histogram presented in [9]. The horizontal axis is measured in units of the numerical average crossing size  $\bar{C}_{KT}$ , i.e.,  $c = C/\bar{C}_{KT}$  (see also below). The solid line is a theoretical probability density distribution of avoided crossings  $P(c)$  obtained from the  $2 \times 2$  model expression, Eq. (2.15), multiplied by  $\pi$  for correct normalization and, importantly, assuming the numerically obtained value of the average avoided crossing. The dotted line represents Eq. (2.6) similarly rescaled. Note that both the solid and the dotted lines fit the numerical data quite well, and the difference between both distributions is quite small.

Let us concentrate on very small avoided crossings first. Figure 2 presents this region of the integrated distribu-

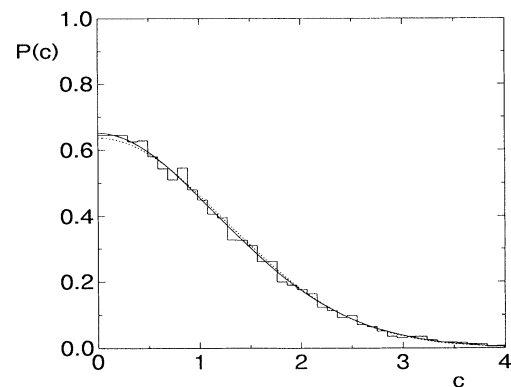


FIG. 1. The normalized histogram of avoided crossings for the kicked-top model Eq. (3.1). Solid and dotted lines compare two theoretical probability-density distributions resulting from Eqs. (2.15) and (2.6), respectively. The horizontal axis is in dimensionless crossings  $c = C/\bar{C}^{KT}$ . Both theoretical distributions are expressed in respect to numerically found mean crossing. The data correspond to  $j = 50$  odd-parity tops with  $k = 10, 11, \dots, 20$  and the parameter  $\lambda = p \in [1.9, 2.6]$  interval.

tion  $D(c)$  in more detail. In panel (a), the solid curve represents the final numerical result obtained with the hyperbola fit while the dotted line corresponds to the parabola fit. The similar curves in panel (b) are obtained with the diagonalization step twice as large. The solid, almost-straight line for the presented range of  $c$  values is the low- $c$  part of the integrated theoretical distribution, while the dashed line corresponds to the integrated probability distribution resulting from Eq. (2.6). Note how with the decreasing step size the apparent hole in the numerical integrated distribution of crossings disappears, with the hyperbola fit results being much better converged than the parabola fit distribution. The region shown in the panels corresponds to 2% of the total number of 11 900 crossings, thus the deviations between the theoretical “lines” and the converged hyperbolic fit result [solid line in panel (a)] are mainly of statistical origin. As exemplified for other systems below, decreasing the step size in diagonalization even more would yield the disappearance of the spurious parabolic hole. Already the presented results show that once a proper numerical pro-

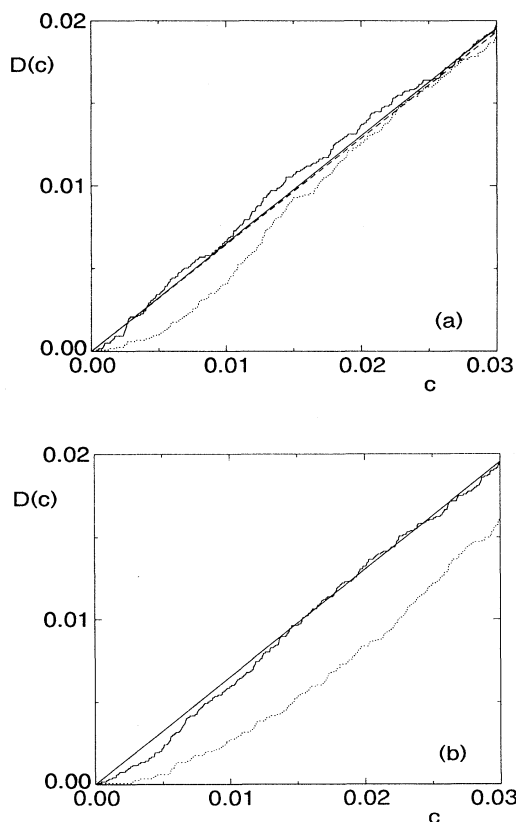


FIG. 2. (a) Detail of Fig. 1: small-avoided-crossing integrated distribution obtained with the hyperbola fit (solid curve) and with the parabola fit (dotted curve). Almost-straight solid and dashed lines correspond to the theoretical integrated distributions resulting from Eqs. (2.15) and (2.6), respectively. (b) reveals the larger “hole” obtained with twice larger step between successive diagonalizations. For the discussion see text.

cedure is applied, the numerical data for kicked top are well described by the theory.

The careful reader has noticed that up until now we have evaded the comparison between the numerically obtained value of the average crossing size  $\bar{C}_{KT}$  and the value predicted by the two-level model (see above),  $\bar{C}_O \approx 0.4142$ . The theoretical curves have been drawn assuming the numerically obtained value which, for the kicked-top model is  $\bar{C}^{KT} = 0.5101$ . Clearly the relatively large difference between  $\bar{C}^{KT}$  and  $\bar{C}_O$  shows that the  $2 \times 2$  model cannot correctly describe large crossings. This is to be expected since, in a fully chaotic region, only the small crossings may be treated as isolated, and only for them will the two-level model be accurate.

## 2. Random-matrix model of level dynamics

Up until now the numerical test of crossing distributions has been performed for the kicked-top model only ([9] and above for the orthogonal universality class). Here we present the results of such a comparison for a “generic” model of autonomous system. The model, based on the random-matrix simulation of the parametric dependence on  $\lambda$  given by Eq. (2.12), has been introduced in I for the purpose of the curvature distributions analysis. Referring the reader to I for details, let us mention only that the matrices  $H_1$  and  $H_2$  are generated in this model from the ensemble of random matrices appropriate for the universality class considered. Let us discuss here the GOE case in which we shall pay particular attention to the problem of numerical convergence of the results. The results for other universality classes will be presented later. The numerical procedure adopted for finding the avoided crossings is the same as the one used above for the kicked top.

Figure 3 presents the results for the GOE model with  $N = 50$  levels on the full scale. The main part shows

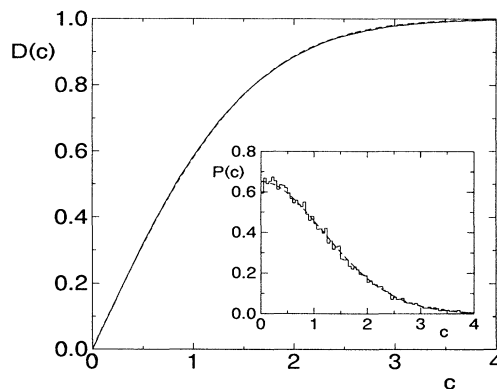


FIG. 3. The integrated probability distribution of avoided crossings  $D(c)$  for the GOE random dynamics compared with the theoretical distribution resulting from Eq. (2.15) shown by the dashed line. The inset shows the comparison of the normalized histogram with the corresponding theoretical probability-density distribution based on Eq. (2.15). Avoided crossings are measured in units of the numerically obtained mean crossing.

the integrated distribution of avoided crossings while the dashed line gives the integrated probability distribution  $D(c)$ . On this scale, the  $2 \times 2$  theory represents the results quite well if expressed in terms of the numerically found value of the mean crossing. The histogram presents the numerical, converged results in unit of the mean crossing  $\bar{C}^{\text{GOE}} \approx 0.5232$  (in unit of the mean spacing), i.e., a value slightly, but significantly, larger than  $\bar{C}^{\text{KT}}$ . To avoid the effect of the boundaries for finite-dimensional matrices, only the levels in the interval  $[-0.5, 0.5]$  have been taken for the analysis; they were unfolded according to the semicircle law, which as tested beforehand, well approximates the average density of states for  $N = 50$ . The total number of crossings obtained is 21 440. It has been tested that the average crossing is reasonably insensitive to the interval of levels taken, e.g., for the  $[-0.7, 0.7]$  interval, the average crossing is 0.5230 mean spacing out of 27 500 crossings. The dashed line in Fig. 3 is the theoretical probability density distribution obtained from Eq. (2.15) (as in the kicked-top case, we use the numerically obtained value of the average crossing size).

The integrated probability distributions are presented in Fig. 4. Only the most interesting, small-crossing regime is presented, as the plot of the fully integrated distribution, similar to the one presented in Fig. 1, is “too good”—the numerical data coincide with the theoretical integrated distribution so the latter are not visible.

Note in Fig. 4 that the fully converged (one “imaginary”—see above—crossing size out of more than 20 000 crossings) hyperbola fit results show quite good agreement with the theoretical dashed line for small crossings while the parabola fit dotted line reveals still a quite small “hole.” The spurious-hole effect appearing while using the parabola fit is exemplified in the inset where three solid lines show the results obtained for different diagonalization step size. The curve closest to the theoretical prediction corresponds to the smallest step and is the same as the dotted line in the main panel.

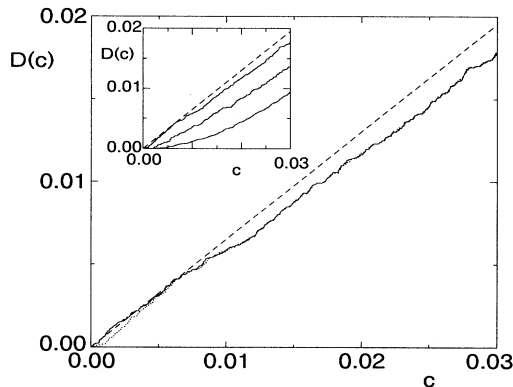


FIG. 4. Detail of the small-crossing integrated distributions. Main panel: the converged hyperbola fit results (solid curve) compared with the results obtained using the parabola fit (dotted curve). Dashed line represents the theoretical prediction. The inset shows three parabola fit distributions, the diagonalization step decreases from the bottom curve to the top curve.

The similar results presented for the kicked top in the previous part and for the GOE model provide the convincing evidence for the fact that the hole reported in previous calculations has been a spurious effect. Let us, however, discuss also other systems studied in [8].

### 3. The Africa billiard

The data for this system have been kindly made available to us by Dr. Goldberg. For the description of the system the reader is referred to [8]. In the original work [8] the authors could not compare the data with the theory [9], which came a bit later, and they restricted themselves to the small crossings limit. The data set contains 725 avoided crossings. The normalized histogram together with the theoretical probability density distribution resulting from Eq. (2.15) is presented in Fig. 5. The relatively small number of avoided crossings has enforced a relatively large bin size for a reasonable comparison. In such a situation much more meaningful is the comparison of the integrated probability distribution  $D(c)$  presented in Fig. 6. The solid smooth curve gives the theoretical prediction and shows quite good agreement with the data, particularly for the smallest avoided crossings. The inset shows the enlarged small-crossing part of the integrated distribution. The solid line connecting the numerically evaluated distribution corresponds to the hyperbola fit, the dotted line to the parabola fit [both data sets have been obtained by Goldberg, the calculations with the hyperbola fit expression, Eq. (3.2), have been performed on our request]. It turns out that the step size assumed in calculations has been so small that the deviation between hyperbola and parabola results is quite small. It is quite clear that what had been interpreted originally as a hole is due to some excess over the theoretical line for a bit larger crossings. This excess is probably of the statistical nature, i.e., it results from the relatively small number of avoided crossings available for this system.

Let us note that the numerical value of the average crossing obtained for the Africa billiard system is  $\bar{C}^{\text{Afr}} \approx$

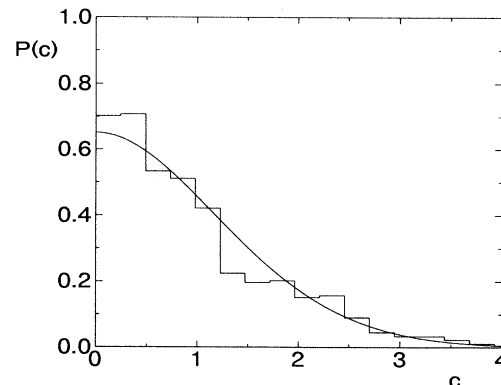


FIG. 5. The normalized histogram of 725 avoided crossings for the Africa billiard system (numerical data courtesy of Goldberg). The solid line is the theoretical prediction based on Eq. (2.15).

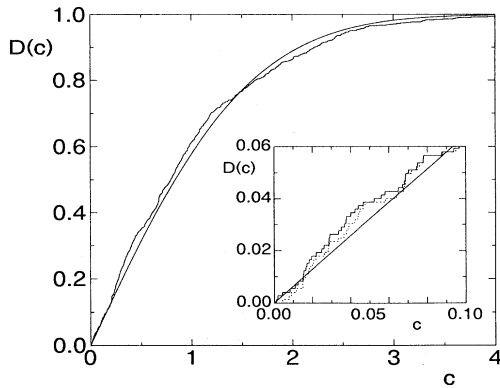


FIG. 6. The integrated probability distribution of avoided crossings for the Africa billiard system (data courtesy of Goldberg) compared with the theoretical prediction. The inset shows the small-crossing region in which the hyperbola fit (solid line) results are compared with the parabola fit results (dotted line). For discussion see text.

0.49 mean spacings, i.e., smaller than in the orthogonal kicked-top model but considerably larger than the  $\bar{C}_O$  value obtained from two-level model considerations. The average crossing seems *not* to be a universal quantity; we shall come back to this point in detail later.

#### 4. The magnetized hydrogen atom

The original eigenvalue data on which the calculation reported in [8] was based were made available to us courtesy of Goldberg. We have analyzed them using both the hyperbola fit and the parabola fit; the results are presented in Fig. 7 and compared with the theoretical distribution. Indeed, the pronounced small-crossing hole is visible. Clearly, however, the results of the hyperbola fit differ strongly from the corresponding results obtained using the parabola fit, which indicates that a too-large

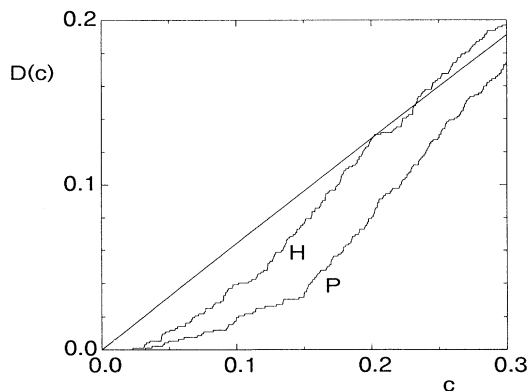


FIG. 7. The original data for the hydrogen atom in a strong magnetic field used in [8] and kindly supplied by Goldberg analyzed using the hyperbola fit (curve denoted by *H*) and by the parabola fit (*P*). Solid line represents the theoretical prediction, for comparison.

step in the diagonalizations has been taken. Also out of a little above 900 avoided crossings, Eq. (3.2) predicted 30 imaginary values which, as discussed in detail while treating the kicked-top model, is another indication of the too-large step taken.

We have, therefore, performed an independent calculation of the avoided crossings for this system. The calculations have been done in the same interval in which the curvature distribution has been studied in I. Therefore, for more details on the diagonalization procedure we refer the reader to I, as well as to the general reviews [16, 17] for more information about this “standard model” of quantum chaos.

In the studied parameter and eigenvalue range, corresponding to a fully chaotic motion, more than 3000 avoided crossings have been found. The value of the average crossing found (in the unit of mean spacing) is  $\bar{C}^{\text{hyd}} \approx 0.420$ , much closer to the two-level model prediction than for other systems. Figure 8 shows the integrated probability distribution, obtained numerically, by a solid line (as in the other plots we use a dimensionless crossing size  $c = C/\bar{C}^{\text{hyd}}$ ) and the theoretical integrated distribution, based on Eq. (2.15), as a dashed line. As for other systems studied, once the data are expressed in terms of the numerically found mean crossing, the agreement between the theory and the numerically obtained data is quite impressive. The inset presents the small-crossing behavior in comparison with the theory. No hole is present and the agreement for small crossings is excellent (a nonzero value of the numerical distribution at zero corresponds to four crossings which, as indicated by the hyperbola fit procedure and other precautions used in numerical evaluation of avoided crossings, are too small to be reliably evaluated).

Figure 9 presents the comparison of the theoretical probability-density distribution with the numerically obtained histogram of avoided crossings. The data presented in Figs. 7 and 8 are firm evidence that the RMT [3] correctly describes the small avoided-crossings behav-

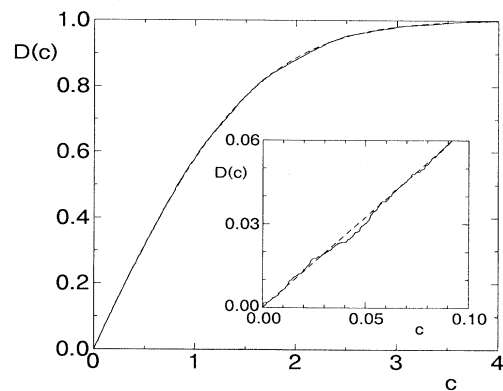


FIG. 8. The integrated probability distribution of avoided crossings  $D(c)$  evaluated independently by us for the same system as in Fig. 7 and compared with the theoretical prediction based on Eq. (2.15). The inset shows the detail of small-crossing behavior. For discussion see text.



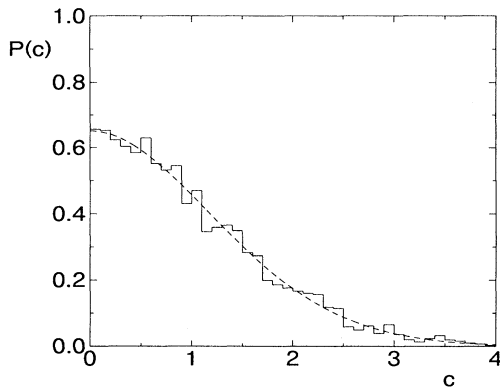


FIG. 9. The normalized histogram of 3063 avoided crossings found for the magnetized hydrogen atom, for the same parameter values as in I, compared with the theoretical probability density distribution (dashed line).

ior. The data (Fig. 9) agree very well with the full distributions found on the basis of the  $2 \times 2$  model.

### B. Other universality classes

As compared with the GOE case, the small crossings are very seldom in both GUE and GSE [as seen from Eqs. (2.7) and (2.11) [9] or the corresponding expressions derived in this paper, Eqs. (2.19) and (2.20)]. This fact has been confirmed in the kicked-top study [9]. The results are not affected by the improvement of the numerical procedure developed here (as small crossings are very rare). Therefore we do not reproduce the results [9] for other universality classes here [obtained with an appropriately modified version of the evolution operator, Eq. (3.1)], especially as similar agreement between the theory and the numerical experiment is obtained in the model of the autonomous system studied below.

To this end we use again the same RMT model described already above (see also I). Figure 10 presents the numerical histogram obtained for the unitary sys-

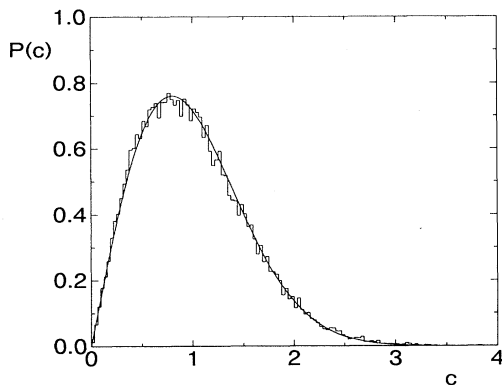


FIG. 10. The theoretical distribution of avoided crossings versus the numerically obtained data for the GUE random dynamics model. For further discussion see text.

tem again in the units of the numerically obtained mean crossing value  $\bar{C}^{\text{GUE}} = 0.638$ . More than 37 000 crossings have been collected, again from the  $[-0.5, 0.5]$  interval. The histogram obtained is fitted quite well by a solid line, which corresponds to the Wigner-like formulas Eq. (2.7). Exactly the same expression results from Eq. (2.19) if the latter is properly normalized and expressed in terms of the average crossing. Let us stress that, as in the GOE case, the numerical average crossing obtained exceeds the  $2 \times 2$  model prediction  $\bar{C}_U \approx 0.555$  (in units of the mean spacing), although the relative difference is a bit smaller.

The similar comparison for the GSE model system is presented in Fig. 11. The dotted line gives the theoretical probability-density distribution obtained from Eq. (2.20) and expressed in terms of the average crossing. The numerical data are rescaled to the same units  $c = C/\bar{C}^{\text{GSE}}$ , where  $\bar{C}^{\text{GSE}} = 0.7359$  and, as for other universality classes, exceeds the two-level prediction  $\bar{C}_S = 0.6768$ . The dashed line corresponds to Eq. (2.11) [9]. Note that as for other universality classes the difference between the predictions given in [9] and the present model based on a canonical ensemble which correctly includes “unfolding” is very small if both corresponding expressions are expressed in terms of the average crossing.

To complete our study of RMT model dynamics we may discuss the case of the partially broken time-reversal invariance. We have not derived the appropriate formulae in the statistical-mechanics formalism although it is quite easy—one must assume only the different  $\beta$  values for the real and imaginary parts of  $L_{12}$  in the Gibbs measure, Eq. (I.3.6). The experience with all three universality classes considered above shows that the difference between the  $2 \times 2$  RMT expressions of [9] and the refined approach proposed here are very small if the theoretical formulas are expressed in the units of the average crossing. Thus it is sufficient to compare the numerical data obtained with the corresponding expression, Eq. (2.9).

To obtain the crossings numerically for a partially broken time-reversal invariance case, we have to modify accordingly the way in which the random matrices  $H_1$  and  $H_2$  in (2.12) are generated, as the description given in I

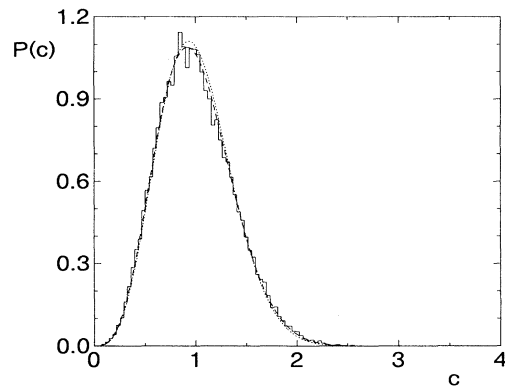


FIG. 11. GSE random-matrix model dynamics. The histogram compared with the theoretical probability density as resulting from Eqs. (2.20) (dotted line) and (2.11) (dashed line).

is valid for pure cases only. The modification is a minor one, namely the symmetric and the asymmetric matrices yielding  $H_i$  (see I) are generated assuming different variances of the random normal distribution, according to Eq. (2.8). Otherwise the crossings are found by the similar procedure, already described. It is probably good to repeat, at this point, that we do *not* consider the transition from one universality class to the other with the change of the parameter  $\lambda$ . On the contrary, we assume that  $\lambda$  changes does not affect the symmetry properties of our system.

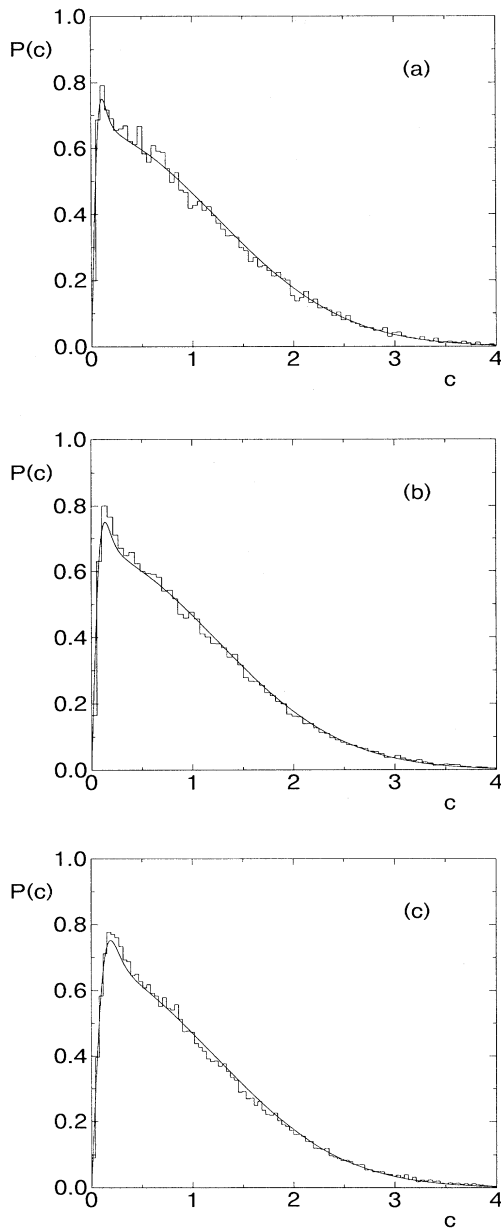


FIG. 12. GOE-GUE transition system. (a)–(c) correspond to the  $N = 25, 50,$  and  $100$  models, respectively. Solid lines represent fitted theoretical distribution Eq. (2.9). For details see text.

In [9] we have studied the different degree of the partial time-reversal invariance breaking by modifying  $\alpha$  in Eq. (2.8). Here we study another interesting effect occurring when we compare the results obtained for matrices of different size  $N$ , keeping  $\alpha$  at a constant value  $\alpha = 0.0001$ . Figure 12 shows the numerical data obtained for  $N = 25, 50,$  and  $100$  in panels (a), (b), and (c), respectively. One notices that the deviation from the GOE behavior, for a fixed value of  $\alpha$ , increases with increasing  $N$ . This is in agreement with study of level-spacing GOE-GUE transition statistical behavior [14]. Also the average crossing values increased with increasing  $N$ . Clearly, as  $\alpha$  is the only parameter in the theoretical expression, Eq. (2.9) (expressed in terms of the average crossing), the  $2 \times 2$  formula cannot describe the observed  $N$ -dependent behavior without some modification. Therefore we have made  $\alpha$  a free parameter and fitted Eq. (2.9) to each data separately. The solid lines in the panels correspond give a results of the fit which yields  $\alpha_{25} = 0.0025$ ,  $\alpha_{50} = 0.004$ , and  $\alpha_{100} = 0.008$ . Note that, adapted in such a way, expression (2.9) reproduces the numerical data quite well. Also the values of  $\alpha_N$  show an expected trend differing more and more from the two-level value with increasing  $N$ .

#### IV. CONCLUSIONS

In this paper an extensive comparison of the theoretical distributions of the avoided crossings, obtained in the two-level RMT model with numerical data for various physical systems as well as for a random model of dynamics, has been presented. It has been found that the theoretical distributions resulting from the two-level model correctly describe the avoided-crossing statistical behavior once the numerical data are expressed in terms of the mean crossing value for all three universality classes of systems. More importantly the discrepancy between the RMT and the previous numerical results concerning the relative number of small avoided crossings for the orthogonal class has been shown to be due to the inaccuracies in the numerical procedures adopted in [8, 9].

On the other hand, significant deviations between the mean crossing value as predicted by the two-level model,  $\bar{C}_O \approx 0.4142$  (for unit mean spacing), and the values obtained for different physical models have been found. Moreover, the numerical data indicate clearly that the mean crossing to the mean spacing ratio is a system-dependent, i.e., a nonuniversal, property. Let us recall the values obtained for the mean crossing (all quoted in the unit of a corresponding mean spacing) for the systems of the orthogonal universality class, most important for applications. For a purely random dynamics we obtained  $\bar{C}^{\text{GOE}} \approx 0.5232$ . The kicked-top model gave  $\bar{C}^{\text{KT}} \approx 0.5101$ , the Africa billiard  $\bar{C}^{\text{Afr}} \approx 0.49$ , while the magnetized hydrogen atom yielded  $\bar{C}^{\text{hyd}} \approx 0.420$ .

While the number of systems studied does not allow us to draw definite conclusions, the numbers presented are quite suggestive. The decrease below the RMT limiting value towards the two-level model value obviously indicates that the isolated two-level avoided crossings become statistically significant in a given system. Such a

narrow avoided crossing may appear only if the states involved are very differently localized. This, in a natural way, leads us to associate the size of the mean crossing with the degree of scarring [13] in the system. This correlates well with the fact that the smallest average crossing has been obtained for a strongly scarred magnetized hydrogen atom [16], while the largest among the physical models studied for the kicked top, for which the scarring, although present [18], is quite small. To validate the usefulness of the proposed statistical measure of scarring further, studies of avoided crossings distributions in other physical systems (e.g., in the stadium billiard [13]) are necessary.

The above interpretation correlates well with the nonuniversal behavior of the small-curvature distribution as found in [19] and discussed in more detail in I. In particular a nice correlation exists with the tentative classification of the physical systems with respect to the degree of scarring based on the small-curvature behavior (of course within the limitation of a relatively small number of systems studied). There is, however, a significant difference too. While the small curvatures are affected by the scarred states behavior “in between” the avoided crossings, the present measure, by definition, comes from the region leading to large curvatures. This supports to some extent, as indication was given while interpreting the data for the stadium billiard in I, that the large-curvature tail may also show a nonuniversal behavior. Certainly, there may be much more information available in the curvature distributions, avoided-crossing distributions, and other statistical measures describing the parametric motion of the levels than this explored in I and here. Further studies, let us mention again, for a wide variety of systems are needed.

Let us finish the study of avoided-crossing distributions with a word of caution. As indicated by the “spurious-hole” effect, evaluations of the small avoided crossings require particular attention. Also, the theoretical expressions given here are valid provided the corresponding classical mechanics is fully chaotic in a full interval of the changed parameter. In the case of the mixed chaotic-regular dynamics, the very small avoided crossings will be much more abundant. This fact is illustrated in Fig. 13, where for the kicked-top model we have investigated the avoided crossings in the domain of the parameter values in which small islands of regularity exist classically. Note the drastic change of the shape of the histogram. The solid line corresponds to a Poisson distribution and is drawn to guide the eye. We have to stress

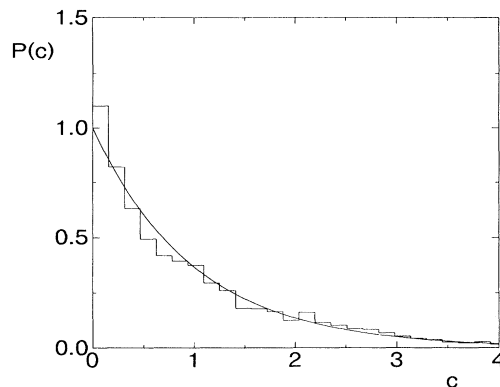


FIG. 13. Normalized histogram of avoided crossings for the kicked top that show classically small islands of regular behavior. Solid line represents the Poisson distribution and is drawn to guide the eye. The data correspond to the  $j = 50$  odd-parity top with  $k = 10, 11, \dots, 20$  and the parameter  $\lambda = p \in [2.7, 2.8]$  interval—compare with Fig. 1. See text for the discussion.

that the level-spacing histograms obtained for the same values of the parameters show only very slight deviations from the Wigner surmise. The study of avoided-crossing distribution in the case presented in Fig. 13 requires, for the reasons given already above, particular attention and very tiny steps between successive diagonalizations, and is, therefore, quite time consuming.

#### ACKNOWLEDGMENTS

This paper profited very much from the outstanding cooperation of Dr. Joel Goldberg, who has not only supplied us with the data used in [8] but also calculated for us the avoided crossings in the Africa billiard system using the hyperbola fit. We thank Dr. Goldberg very deeply. We are grateful to Professor Oriol Bohigas and Professor Fritz Haake for interesting discussions. J.Z. thanks his colleagues at the Laboratoire de Spectroscopie Hertzienne for hospitality and the Ministère de la Recherche et de la Technologie for the financial support. Support of the Polish Committee of Scientific Research under Grant No. 200799101 (J.Z. and M.K.) is acknowledged. Laboratoire de Spectroscopie Hertzienne de l’Ecole Normale Supérieure et de l’Université Pierre et Marie Curie is “Unité Associée 18 du Centre National de la Recherche Scientifique.”

\* Permanent address: Instytut Fizyki, Uniwersytet Jagielloński, ulica Reymonta 4, 30-059 Kraków, Poland.

- [1] J. Zakrzewski and D. Delande, preceding paper, *Phys. Rev. E* **47**, 1650 (1993).
- [2] D. W. Noid, M. L. Koszykowski, M. Tabor, and R. A. Marcus, *J. Chem. Phys.* **72**, 6169 (1980).
- [3] M. Wilkinson, *J. Phys. A* **22**, 2795 (1989).
- [4] C. E. Porter, *Statistical Theories of Spectra. Fluctuations* (Academic, New York, 1965).

- [5] M. L. Mehta, *Random Matrices* (Academic, New York, 1991).
- [6] F. Haake, *Quantum Signatures of Chaos* (Springer, Berlin, 1991).
- [7] O. Bohigas, in *Chaos and Quantum Physics*, 1989 Les Houches Lectures Session LII, edited by M.-J. Giannoni, A. Voros, and J. Zinn-Justin (North-Holland, Amsterdam, 1991), p. 87.
- [8] J. Goldberg and W. Schweizer, *J. Phys. A* **24**, 2785

- (1991).
- [9] J. Zakrzewski and M. Kuś, *Phys. Rev. Lett.* **67**, 2749 (1991).
- [10] M. Kuś, R. Scharf, and F. Haake, *Z. Phys. B* **66**, 129 (1987).
- [11] F. Haake, M. Kuś, and R. Scharf, *Z. Phys. B* **65**, 381 (1987).
- [12] R. Scharf, B. Dietz, M. Kuś, F. Haake, and M. V. Berry, *Europhys. Lett.* **5**, 383 (1988).
- [13] E. Heller, *Phys. Rev. Lett.* **53**, 1515 (1984).
- [14] G. Lenz and F. Haake, *Phys. Rev. Lett.* **65**, 2325 (1990);
- 67**, 1 (1991).
- [15] I. S. Gradshteyn and I. M. Ryzhik, *Table of Integrals, Series and Products* (Academic, New York, 1980).
- [16] For a review see, e.g., D. Delande, in *Chaos and Quantum Physics* (Ref. [7]), p. 665.
- [17] H. Friedrich and D. Wintgen, *Phys. Rep.* **183**, 37 (1989).
- [18] M. Kuś, J. Zakrzewski, and K. Życzkowski, *Phys. Rev. A* **43**, 4244 (1991).
- [19] T. Takami and H. Hasegawa, *Phys. Rev. Lett.* **68**, 419 (1992).